

Ultrasonic study of the temperature and pressure dependences of the elastic properties of ceramic dimolybdenum carbide (α -Mo₂C)

M. CANKURTARAN

Department of Physics, Hacettepe University, Beytepe, 06532 Ankara, Turkey

E-mail: cankur@hacettepe.edu.tr

S. P. DODD

Department of Physics, University of Bath, Bath BA2 7AY, UK

B. JAMES

DSTL-Chertsey (Armour Group), Chobham Lane, Chertsey, Surrey KT16 0EE, UK

Pulse-echo overlap measurements of ultrasonic wave velocity have been used to determine the elastic stiffness moduli and related elastic properties of ceramic samples of dimolybdenum carbide (α -Mo₂C) as functions of temperature in the range 130–295 K and hydrostatic pressure up to 0.2 GPa at room temperature. The temperature dependences of the shear elastic stiffness (μ) and Young's modulus (E) show normal behaviour and can be approximated by a conventional model for vibrational anharmonicity. The longitudinal elastic stiffness (C_L) increases with decreasing temperature and shows a knee at about 200 K; the decrease in slope below the knee indicates longitudinal acoustic-mode softening. The adiabatic bulk modulus (B^S) is also affected by the mode softening below 200 K. The values obtained for the acoustic Debye temperature (Θ_D) for ceramic α -Mo₂C agree well with the thermal Debye temperature determined previously from heat capacity measurements. The velocities of both the longitudinal and shear ultrasonic waves in ceramic α -Mo₂C increase approximately linearly with pressure: both the long-wavelength longitudinal and shear acoustic modes stiffen under pressure. The values determined at room temperature for the hydrostatic-pressure derivative $(\partial\mu/\partial P)_{P=0}$ of the shear stiffness is similar to those found for ceramic TiC and TaC; while $(\partial C_L/\partial P)_{P=0}$ and $(\partial B^S/\partial P)_{P=0}$ have large values, possibly due to the defect microstructure of ceramic α -Mo₂C.

© 2004 Kluwer Academic Publishers

1. Introduction

Transition metal carbides are compounds of great technological and scientific interest. They combine properties of metals and covalent compounds, such as great hardness, good chemical and mechanical stability and resistance to corrosion, a high melting point, high electrical and thermal conductivity and brittle-to-ductile transitions at high temperatures [1–3]. Dimolybdenum carbide (Mo₂C) belongs to the group VI transition metal carbides. Previous studies have shown that it has metallic electrical properties with a superconducting transition temperature of 9.7 K [4]. Mo₂C has potential uses in diffusion barriers and electrical connections in microelectronics [5, 6]. At temperatures above 1960°C, Mo₂C adopts a disordered, hexagonal L'3-type structure (space group $P6_3/mmc$, $Z = 1$), in which the molybdenum atoms form a hexagonal close packed array and the carbon atoms occupy one half of the octahedral interstitial sites in a random way [7–10]. Transitions are observed to ordered structures upon cooling. An ϵ -Fe₂N-type structure (space group $P\bar{3}m1$, $Z = 2$)

is present between 1960 and 1350°C, and below this temperature the structure changes to the ζ -Fe₂N type (space group $Pbcn$, $Z = 4$) and is designated the α -phase of Mo₂C [7]. The α -phase is the only stable structure under ambient conditions with the carbon atoms occupying one half of the interstitial sites in an ordered way [7–10]. This phase is obtained by ordering the carbon atoms in the cell corresponding to the orthorhombic (o) setting of L'3-type Mo₂C (hex) with $a_o = c_{\text{hex}}$, $b_o = 2a_{\text{hex}}$, $c_o = \sqrt{3}a_{\text{hex}}$ [7–9]. The structure of this form has been refined by neutron diffraction [8, 9].

A recent theoretical study [10] has predicted that α -Mo₂C has a high bulk modulus, but is less hard in comparison to cubic transition-metal carbides (e.g., TiC and TaC). However, despite the technological importance of α -Mo₂C, understanding of the elastic properties of its ceramic form is sparse. Previously, Young's modulus of ceramic Mo₂C has been investigated at room temperature [1–3, 5, 11–15] and in a temperature range from 103 to 1373 K [15]. Recently, Kral *et al.* [16] compiled the available data for the room temperature

Young's modulus of Mo_2C , but the data was scattered over a wide range from 228 to 534 GPa. While studying the bonding characteristics of molybdenum carbide, Toth *et al.* [17] observed that there was a marked disagreement (of around 300 K) between the Debye temperature obtained from sound velocity measurements on single-crystal Mo_2C [18, 19] and that derived from low temperature heat capacity data [20]. Chang *et al.* [21] argued that the sound velocity data for Mo_2C reported in the literature [18, 19] may be in error, and noted that independent sound velocity measurements are required (see also [1]).

The present ultrasonic study of the elastic and nonlinear acoustic properties of ceramic $\alpha\text{-Mo}_2\text{C}$ has been largely motivated by the need for accurate measurements of the effects of temperature and hydrostatic pressure on the velocities of longitudinal and shear ultrasonic waves in this material. These measurements are essential for design purposes in technological applications and scientific investigations of the dynamic response of the material to applied pressure. Ultrasonic wave velocity measurements on ceramic $\alpha\text{-Mo}_2\text{C}$ have been extended from room temperature down to 130 K. To assess the nonlinear acoustic properties of this ceramic, ultrasonic wave velocities have been measured as a function of hydrostatic pressure up to 0.2 GPa at room temperature. The outcome of this experimental work has been the determination of the technological elastic stiffness moduli and related elastic properties of this ceramic and how they vary with temperature and hydrostatic pressure. The elastic stiffnesses of a material determine the slopes of the acoustic phonon dispersion curves in the long-wavelength limit; their hydrostatic-pressure dependences provide information on the shift of the acoustic mode energies with compression.

2. Experimental procedures

The Mo_2C ceramic used in this work was supplied by Testbourne (U.S.A.) and fabricated using a hot-pressing technique. An X-ray diffraction examination (Fig. 1) showed that the ceramic consisted of a single-phase ($\alpha\text{-Mo}_2\text{C}$) and there was no preferred orientation. The lattice parameters for the hexagonal unit cell, determined from the X-ray data, were $a_{\text{hex}} = 2.9997 \pm 0.0060 \text{ \AA}$

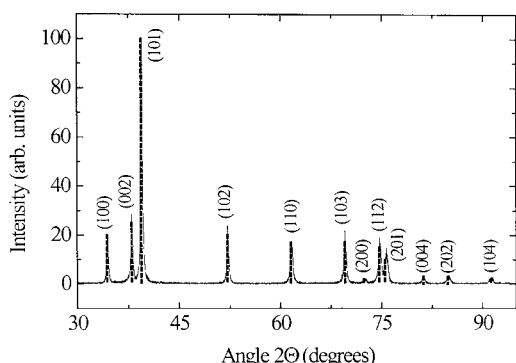


Figure 1 X-ray diffraction pattern for ceramic $\alpha\text{-Mo}_2\text{C}$. The vertical dashed lines denote $\alpha\text{-Mo}_2\text{C}$ powder diffraction standard. The lines are indexed in accordance with the hexagonal subcell described in the introduction.

and $c_{\text{hex}} = 4.724 \pm 0.010 \text{ \AA}$, which are in good agreement with those reported in the literature [4, 7–10, 22]. The above hexagonal cell parameters correspond to a subcell of the actual orthorhombic unit cell of this stable $\zeta\text{-Fe}_2\text{N}$ type form of Mo_2C [8–10]. An electron microprobe analysis revealed the presence of 0.94 wt% oxygen in the $\alpha\text{-Mo}_2\text{C}$ ceramic. Spectroscopic analysis of the starting powders used in the fabrication of this ceramic revealed the presence of small amounts of impurities: $\alpha\text{-Mo}_2\text{C}$ powders contained, by weight, <0.01% calcium and <0.03% titanium. The sample density ρ ($=7840 \pm 30 \text{ kgm}^{-3}$) was measured by Archimedes' method using distilled water as a flotation fluid. The density of the sample is 86% of the theoretical density (9120 kgm^{-3}) of pure $\alpha\text{-Mo}_2\text{C}$ [2, 14, 18]. SEM analyses showed that the pores are irregularly shaped (with a maximum size less than about $10 \mu\text{m}$) and randomly distributed in the ceramic.

To further characterise the fundamental properties of ceramic $\alpha\text{-Mo}_2\text{C}$, electrical resistivity has been measured in the temperature range from 300 to 900 K, in an atmosphere of flowing dry nitrogen. The electrical resistivity of $\alpha\text{-Mo}_2\text{C}$ has not been extensively studied. Only one study exists on the measurement of electrical resistivity as a function of temperature, which was performed in the range 4.2–300 K [4]. The present results for the temperature dependence of the electrical resistivity of ceramic $\alpha\text{-Mo}_2\text{C}$ (Fig. 2) complement those reported previously [4]. Two ceramic bars with approximate dimensions $1.5 \times 1.5 \times 10 \text{ mm}$ were cut from the same block as the ultrasonic sample. To measure the resistance of the bar sample, the standard four-point probe method was used, and the samples were supplied with d.c. current between 50 and 70 mA. The main error (about 4%) in resistance was that incurred in determining the contact separation. Errors in the resistivity calculations appearing because of contact placement and sample dimensions were tested by a Poisson equation calculation [23], and were found to be negligible.

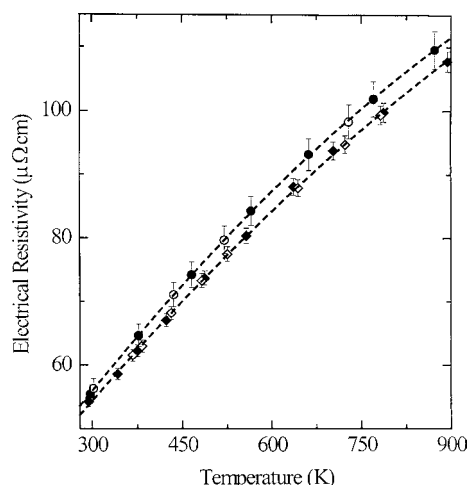


Figure 2 Temperature dependence of the electrical resistivity for ceramic $\alpha\text{-Mo}_2\text{C}$, measured using the four-point probe d.c. technique. The circles (diamonds) correspond to sample 1 (sample 2). The filled (open) symbols correspond to measurements made with increasing (decreasing) temperature. The dashed lines are second-order polynomial fits to the experimental data.

Other errors such as thermal voltages were removed by taking forward and reverse current measurements. Averaging the results of room temperature resistivity measurements on two bar samples of ceramic α -Mo₂C generated a value of $55 \pm 2 \mu\Omega\text{cm}$. Although the room temperature resistivity value should be affected by the porous microstructure of the samples, good agreement is found between the resistivity determined here and that ($\sim 57 \mu\Omega\text{cm}$) measured previously [4] on a 97.4% dense polycrystalline α -Mo₂C sample. A higher value of $71 \mu\Omega\text{cm}$ was quoted [2, 3] without giving information about the sample characterisation. Lucazeau *et al.* [6] determined a value of $80 \mu\Omega\text{cm}$ for the room temperature electrical resistivity of Mo films deposited on polycrystalline diamond films, and noted that the higher resistivity may result from the occurrence of carbon at the grain boundaries. The α -Mo₂C ceramic shows metallic-like electrical behaviour on increasing temperature (Fig. 2); the average temperature derivative of electrical resistivity, evaluated at room temperature, is $113 \text{ n}\Omega\text{cmK}^{-1}$. This value is smaller than $176 \text{ n}\Omega\text{cmK}^{-1}$ determined previously [4] in the temperature range below 300 K. The downward curvature of the electrical resistivity versus temperature curve suggests that the electrical resistivity of ceramic α -Mo₂C is progressing to saturation at high temperatures. This electrical behaviour is similar to previously published results of electrical resistivity measurements on a number of group IV and V transition-metal carbides, including TaC, TiC, V₆C₅ and ZrC [24–27]. Transition metal carbides exhibit a tendency toward resistivity saturation at elevated temperatures. Theoretical models have been proposed to explain this behaviour [4, 26].

An ultrasonic sample, in the shape of a parallelepiped with approximate dimensions $10 \times 8 \times 8 \text{ mm}$, which was large enough for precision measurements of ultrasonic wave velocities, was cut and polished with three pairs of faces, flat to surface irregularities of about $3 \mu\text{m}$ and parallel to better than 10^{-3} rad . To generate and detect ultrasonic pulses, X- or Y-cut (for longitudinal and shear waves, respectively) 10 MHz quartz transducers were bonded to the specimen using Nonaq stopcock grease for low temperature experiments. Dow resin was used as bonding material for pressure experiments. Ultrasonic pulse transit times were measured using a pulse-echo overlap system [28], particularly well suited to the determination of pressure- or temperature-induced changes in velocity. A correction was applied to the ultrasonic wave velocity for multiple reflections at the sample-transducer interface [29]. The temperature dependence of ultrasound velocity was measured in the temperature range 130–295 K using a closed-cycle cryostat. At lower temperatures, thermal expansion differences between sample, bond and transducer caused the ultrasonic signal to be lost; a number of bonding agents were tried, but none gave satisfactory results. The dependence of ultrasonic wave velocity upon hydrostatic pressure was measured at room temperature (295 K). Hydrostatic pressure up to 0.2 GPa was applied in a piston and cylinder apparatus using silicone oil as the pressure transmitting medium. Pressure was measured using the change in resistance of a pre-calibrated

manganin wire coil (fixed on the sample holder) inside the pressure cell. Pressure induced changes in the sample dimensions were accounted for by using the “natural velocity (W)” technique [30].

3. Elastic properties at room temperature

The velocities of longitudinal (V_L) and shear (V_S) 10 MHz ultrasonic waves propagated in ceramic α -Mo₂C at room temperature are given in Table I. This small grained polycrystalline ceramic can be treated as an isotropic material, which has two independent elastic stiffness moduli $C_L (= \rho V_L^2)$ and $\mu (= \rho V_S^2)$. The elastic anisotropy was checked by measuring both longitudinal and shear wave velocities in the sample at room temperature for three orthogonal wave propagation directions: the α -Mo₂C ceramic was found to be elastically isotropic. Discrepancies in the measured sets of longitudinal and shear ultrasonic velocities amounted to differences of around 0.5% in the longitudinal and 2% in shear mode velocities. The longitudinal (C_L) and shear (μ) elastic stiffnesses, adiabatic bulk modulus (B^S), Young’s modulus (E), and Poisson’s ratio (σ) have been determined, from the ultrasonic velocity data and sample density, by using the relationships for an isotropic solid (see for instance [33]). The average longitudinal and shear mode velocities obtained from the data measured to assess the elastic isotropy of the sample have been used in the calculation of these elastic properties. The acoustic Debye temperature (Θ_D) has been calculated using the relation [34]

$$\Theta_D = \frac{h}{k} \left(\frac{3\rho N_A n}{4\pi m} \right)^{1/3} \left[\frac{1}{3} \left(\frac{1}{V_L^3} + \frac{2}{V_S^3} \right) \right]^{-1/3}, \quad (1)$$

where h is the Planck’s constant, k is the Boltzmann’s constant, ρ is the sample density, N_A is the Avogadro’s

TABLE I The density, porosity, ultrasonic wave velocities, adiabatic elastic moduli and their hydrostatic-pressure derivatives for ceramic α -Mo₂C at 295 K. The raw experimental data for the ceramic sample are given in the first column. Data for the non-porous (void-free) matrix obtained by applying the correction methods developed in [31] (Method-1) and [32] (Method-2) are also given for comparison

Description	Ceramic sample	Non-porous matrix	
		Method-1	Method-2
Density ρ (kgm^{-3})	7840 ± 30	9120	9120
Porosity (%)	14	–	–
Longitudinal wave velocity V_L (ms^{-1})	6257 ± 18	6727	6906
Shear wave velocity V_S (ms^{-1})	3605 ± 40	3926	3905
Longitudinal stiffness C_L (GPa)	306 ± 2	412	434
Shear stiffness μ (GPa)	101 ± 2	140	139
Bulk modulus B^S (GPa)	171 ± 3	225	248
Young’s modulus E (GPa)	253 ± 4	347	351
Poisson’s ratio σ	0.25 ± 0.01	0.243	0.264
Acoustic Debye temperature Θ_D (K)	490 ± 8	560	559
$(\partial C_L / \partial P)_{P=0}$	17.2 ± 0.4		
$(\partial \mu / \partial P)_{P=0}$	1.09 ± 0.02		
$(\partial B^S / \partial P)_{P=0}$	15.7 ± 0.4		

number, n is the number of atoms in the unit formula and m is the molecular weight. The acoustic phonon dispersion curves and hence the ultrasonic wave velocity in transition metal carbides are determined by the interatomic bonding between metal-metal atoms and metal-carbon atoms [1]. Therefore, both the molybdenum atoms and the carbon atoms in the unit cell are included in the calculation of Θ_D . The results obtained for C_L , μ , B^S , E , σ and Θ_D for ceramic α -Mo₂C are summarised in Table I.

The presence of pores in ceramic samples leads to a reduction in the measured ultrasonic wave velocities (and hence the elastic stiffness moduli). To enable a meaningful comparison between the elastic properties of ceramic α -Mo₂C determined in this study and those available in the literature, it is necessary to correct for the effects of porosity on the measured moduli. The correction methods commonly used are those developed for porous or cracked bodies, such as ceramics and rocks, or those for a composite with inclusions (for an overview see [35]). In this study, corrections for the influence of specimen porosity have been made for the room temperature data using the correction methods developed by [31] and [32]. Sayers and Smith [31] extended a self-consistent treatment to the problem of porous materials with porosity up to 30%, based on a multiple-scattering theory developed [36] for propagation of waves through a random assembly of spheres. With their method, Sayers and Smith [31] could obtain the longitudinal and shear mode velocities of ultrasonic waves propagated in a matrix; only the effects of the sample porosity were considered. Cankurtaran *et al.* [32] developed equations to calculate the bulk and shear moduli of the matrix with a theoretical treatment of the wave propagation under pressure in an isotropic solid in which the distribution of pores is uniform. Both the porosity (up to $\sim 30\%$) and the bulk modulus of the pore filling fluid are included in this method of correction. If the specimen is at atmospheric pressure in air or under vacuum, the porosity is the only factor effective in this method. These two correction methods give similar results for the elastic moduli after correction (Table I). Comparison between the ultrasonic data as measured on ceramic α -Mo₂C and those determined for the non-porous (void-free) matrix (Table I) shows that the effect of porosity is to reduce substantially the ultrasonic wave velocity and hence the elastic moduli (C_L , μ , B^S and E) and the acoustic Debye temperature (Θ_D). While, Poisson's ratio (σ) is affected only slightly.

The adiabatic bulk modulus is increased by this correction for the effects of porosity (Table I). However, the bulk modulus estimated for the non-porous matrix of ceramic α -Mo₂C is smaller (by about 19%) than the value (=307 GPa) obtained [10] from high-pressure X-ray powder diffraction measurements on α -Mo₂C at room temperature. *Ab-initio* calculations [10] generated values for the bulk modulus of Mo₂C ranging from 291 to 307 GPa depending on the carbon-ordering pattern. This indicates that, in addition to porosity, other factors such as impurities and possible microcracking at the grain boundaries influence the magnitude

TABLE II Comparison between the Young's modulus of ceramic α -Mo₂C determined in the present work and the data taken from the literature. The symbol (–) means that experimental method not given

Young's modulus (GPa)	Experiment	Reference
253 ± 4	Ultrasonic, pulse-echo overlap	Present work
350	Porosity correction	Present work
216	Sonic method	[11]
533	–	[12]
223	–	[13]
225	–	[13]
534	–	[13]
228	–	[1, 14]
530	Dynamic resonance method	[15]
322	–	[22]
530	–	[2]
230	–	[3]
339.1 ± 33.4	Depth sensing indentation	[5]

of the bulk modulus of ceramic α -Mo₂C used in this study.

The Young's modulus of ceramic α -Mo₂C has been the subject of several experimental investigations. However, the data obtained previously in different experimental studies are scattered over a wide range (Table II). In most cases the sample density was not given and it is not clear whether elastic data are corrected for porosity [16]. The lack of sample characterisation (i.e. impurity content and porosity) in previous studies on Young's modulus of ceramic α -Mo₂C makes it difficult to compare the present data with those available in the literature. The value determined here for the Young's modulus of the non-porous matrix of ceramic α -Mo₂C falls in the range of values (Table II) found by other researchers using different experimental techniques and is in reasonable agreement with that determined by Martinelli *et al.* [5]. In an investigation of the shear strength of solid state bonded SiC-Mo joints, prepared by uniaxial hot-pressing without intermediate materials, Martinelli *et al.* [5] evaluated the Young's modulus of Mo₂C present at the interface, which was formed by diffusion of C into Mo, by depth sensing indentation. The Young's modulus (339.1 ± 33.4 GPa) of this Mo₂C was calculated from the slope of the unloading segments of the load-depth plots. The unusually large error in the value of Young's modulus was attributed [5] to the surface defects such as scratches and voids. In the calculation of internal stresses in ceramic Mo₂C, Stuart and Ridley [22] adopted a value of 322 GPa for Young's modulus, which is an average of the data given in [13].

Vahldiek and coworkers [18, 19] determined the Young's modulus (E) values of single-crystal Mo₂C from microhardness indentation measurements. The experimental method was considered to be accurate to within 10%. Anisotropy in Young's modulus was found and correlated with microhardness anisotropy and the Mo₂C crystal structure. For unannealed Mo₂C single crystals, virtually no elastic modulus anisotropy was found on the (0001) plane, with the average value being $E = 528$ GPa. Along the (2 $\bar{1}$ 10) plane, an average value of $E = 385$ GPa was obtained. A value of

$E = 301$ GPa was derived for the (10 $\bar{1}$ 2) plane. The Young's modulus along the long axis ($\approx c$ -axis) of the Mo₂C crystal was also obtained [19] by an ultrasonic method and determined to be 288 GPa. Along the short axis of the Mo₂C crystal, a value of 566 GPa was determined using the same ultrasonic method, in fair agreement with that calculated from hardness indentations on the (0001) plane.

The acoustic Debye temperature (Table I) determined in the present study for the non-porous matrix of ceramic α -Mo₂C is in reasonable agreement with the results of previous measurements of heat capacity: i.e., 546, 553 and 608 K for thermal Debye temperature [1, 21]. However, these values disagree with the average Debye temperature (=892 K) found [18, 19] for single-crystal Mo₂C, using the mean sound velocities. Vahldiek and Mersol [19] used an ultrasonic attenuation comparator at a frequency of 5 MHz to measure some of the sound velocity values of single-crystal Mo₂C at room temperature. A mean shear velocity $\bar{v}_S = 8620$ ms⁻¹ and a mean longitudinal velocity $\bar{v}_L = 5680$ ms⁻¹ were determined for single-crystal Mo₂C, which gave a mean sound velocity $\bar{v}_m = 6990$ ms⁻¹; \bar{v}_L is much smaller than \bar{v}_S . It appears that the accuracy of previous sound velocity measurements [19] for Mo₂C crystals is questionable, since, in general, the longitudinal wave velocity in solids is larger than the shear wave velocity (see for instance [33]). Although the mean longitudinal velocity \bar{v}_L determined previously for single-crystal Mo₂C is comparable to the longitudinal velocity measured here for ceramic α -Mo₂C, the mean shear velocity \bar{v}_S for single-crystal Mo₂C [19] is extremely large (by a factor of about 2.4) when compared to the shear wave velocity for ceramic α -Mo₂C (Table I). As noted by Chang *et al.* [21] and Toth [1], the discrepancy could be due to inaccuracies in previous measurements of sound velocity in single-crystal Mo₂C.

The elastic moduli of solids provide a measure of the interatomic forces. It is well known that the bulk and Young's moduli for the transition metal carbides are much higher than those of the parent transition metals [1]. The enhanced values of the elastic moduli for the transition metal carbides over the parent transition metals were attributed to the presence of carbon in the lattice, which promotes strong metal-to-carbon and metal-to-metal bonds. This interpretation is in line with current theories of atomic bonding in transition metal carbides [37, 38]. The results of the present ultrasonic study suggest that α -Mo₂C follows the same trend: the Young's modulus of its ceramic form is larger than that ($\cong 320$ GPa) of molybdenum metal [3, 5, 19].

4. Temperature dependence of the elastic stiffness moduli

The variations of longitudinal (C_L) and shear (μ) elastic stiffnesses with temperature for ceramic α -Mo₂C are shown in Fig. 3a and b, respectively. They were obtained from the sample density and the measured velocities of 10 MHz ultrasonic waves propagated in the sample as it was cycled between room temperature and the lowest temperature of measurement. There was no measurable thermal hysteresis in the ultrasonic wave veloc-

ities and no irreversible effects. Corrections on elastic moduli for sample length and density changes are expected to be negligible due to the low thermal expansion of α -Mo₂C [2, 5, 14, 22]. Both C_L and μ increase with decreasing temperature. Although the presence of pores affects the absolute value of elastic moduli, their influence on the temperature dependence should be much less [15, 39]. The temperature dependence of the shear stiffness (Fig. 3b) can be approximated by the conventional model for lattice vibrational anharmonicity [40]:

$$M(T) = M_0[1 - KF(T/\Theta_D)] \quad (2)$$

with

$$F(T/\Theta_D) = 3 \left(\frac{T}{\Theta_D} \right)^4 \int_0^{\Theta_D/T} \frac{x^3 dx}{e^x - 1}. \quad (3)$$

Here M refers to elastic stiffness modulus, and M_0 and K are constants. The Young's modulus also fits Equation 2 but with a slight deviation below 200 K (Fig. 3c). We obtained a value of -140×10^{-6} K⁻¹ for the temperature coefficient of Young's modulus of hot-pressed α -Mo₂C ceramic, which is somewhat larger than that (-110×10^{-6} K⁻¹) found [15] for sintered Mo₂C ceramic, in the temperature range from 103 to 1373 K. Without presenting experimental data, Frantsevich *et al.* [15] noted that ceramic Mo₂C had linear relationship between temperature and Young's modulus.

The longitudinal elastic stiffness C_L of ceramic α -Mo₂C increases normally with decreasing temperature and shows the unusual feature of a change in slope at about 200 K where there is a knee (Fig. 3a). There is a softening below the knee. The longitudinal modulus does not obey the conventional model [40] for vibrational anharmonicity. The bulk modulus B^S also shows a knee (Fig. 3d) arising from the longitudinal acoustic-mode softening. In its ceramic form α -Mo₂C is not as stiff at low temperatures as a theoretical lattice dynamical model developed without including mode softening would suggest. The corresponding decrease in bulk modulus indicates a considerable weakening in the interatomic binding forces. The softening of longitudinal acoustic modes implies incipient lattice instability at low temperatures [41]. Coherent inelastic neutron scattering study [42] of the lattice dynamics of transition metal carbides TaC and HfC showed that superconducting TaC has anomalous dips (softening) in its longitudinal acoustic-mode dispersion curves, whereas non-superconducting HfC does not exhibit such features. The longitudinal acoustic phonon softening leads to an increase in the electron-phonon coupling constant and hence to a high superconducting transition temperature (T_C) for certain stoichiometric carbides including TaC and NbC [24, 42]. The Nb metal, which also exhibits soft modes in its phonon frequency spectrum, has the highest T_C (=9.26 K) of elemental metals [24]. The longitudinal acoustic-mode softening in ceramic α -Mo₂C below about 200 K (Fig. 3a) could be associated with the transition at T_C ($\cong 9.7$ K) [4] from the normal to superconducting state.

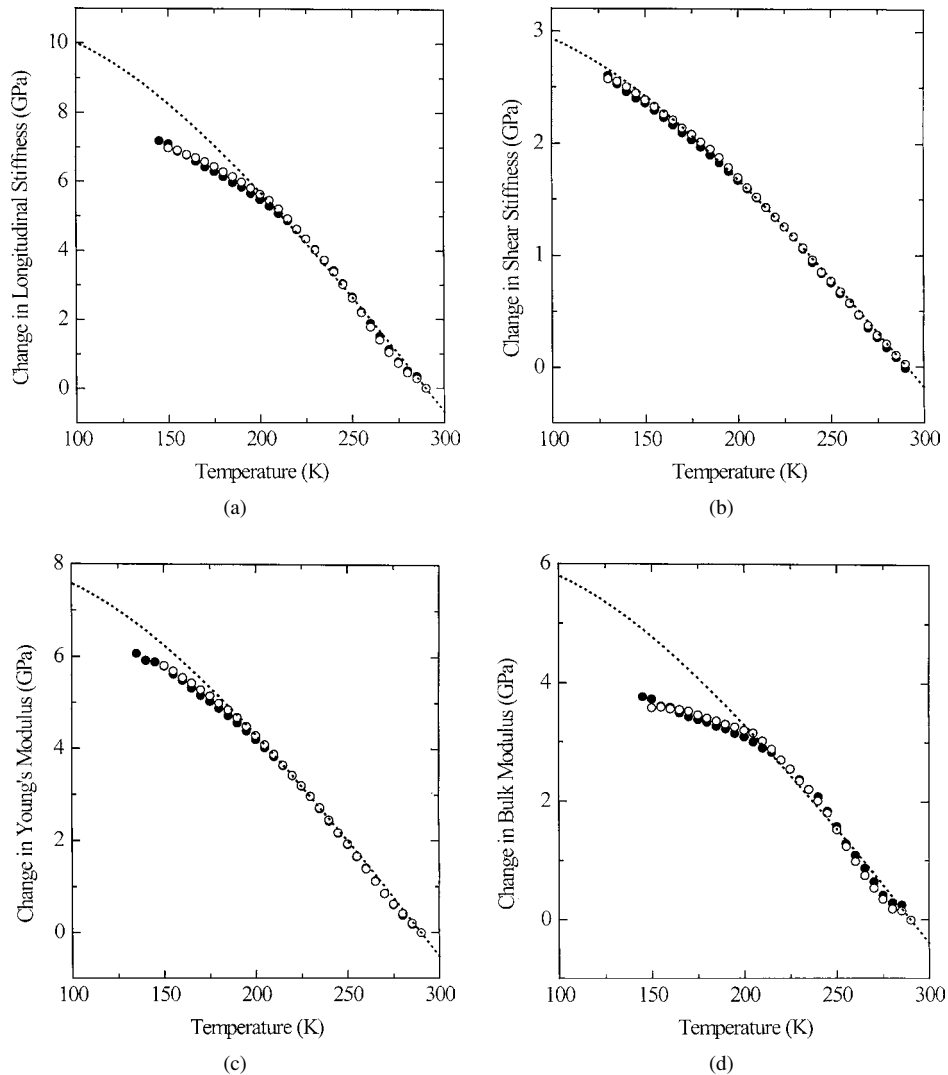


Figure 3 The change of elastic moduli of ceramic α -Mo₂C with temperature ($M(T) - M(290 \text{ K})$): (a) longitudinal stiffness, (b) shear stiffness, (c) Young's modulus and (d) bulk modulus. The filled (open) symbols correspond to measurements made with decreasing (increasing) temperature. The dotted line refers to the elastic modulus calculated by fitting the lattice vibrational anharmonicity model [40] to the experimental data.

The acoustic Debye temperature determined for ceramic α -Mo₂C increases slightly on lowering temperature in accord with stiffening of both the longitudinal and shear wave velocities. Poisson's ratio remains practically constant in the whole temperature range of measurements. This implies that, as the temperature is decreased from room temperature down to 130 K, there is no change in restoring forces associated with the shearing of the lattice. No previous measurements have been reported for the temperature dependences of the longitudinal, shear and bulk moduli, Debye temperature and Poisson's ratio for α -Mo₂C.

5. Hydrostatic-pressure dependences of the ultrasonic wave velocity and elastic stiffness moduli

After the ultrasonic measurements as a function of temperature had been completed, the sample was placed in the pressure cell in order to measure the effects of hydrostatic pressure on ultrasonic wave velocity. The data for the pressure dependence of the velocities of both longitudinal and shear ultrasonic waves propagated in ceramic α -Mo₂C are reproducible under pres-

sure cycling and show no measurable hysteresis effects (Fig. 4). This observation indicates that the α -Mo₂C ceramic does not alter in morphology under pressure cycling up to 0.2 GPa and that there is no relaxation of any residual stress. The longitudinal wave velocity is much more pressure dependent than the shear wave velocity. The velocities of both the longitudinal and shear ultrasonic waves increase approximately linearly with pressure. This is normal behaviour: both the long-wavelength longitudinal and shear acoustic modes stiffen under pressure. No indication of mode softening in the measured pressure range was found. The scatter in the shear mode data is negligible when compared with that in the longitudinal mode results (Fig. 4); hence it would seem that the scatter in the longitudinal wave velocity is a consequence of a volume effect. The source of the scatter in the longitudinal wave velocity could be because the local environments containing pores (and other microstructural defects such as slip lines, veining structure and dislocations [7, 19]) would be affected differently, when increasing pressure is applied to the ceramic sample.

The hydrostatic-pressure derivative $(\partial M/\partial P)_{P=0}$ of elastic stiffness (M) has been obtained from the

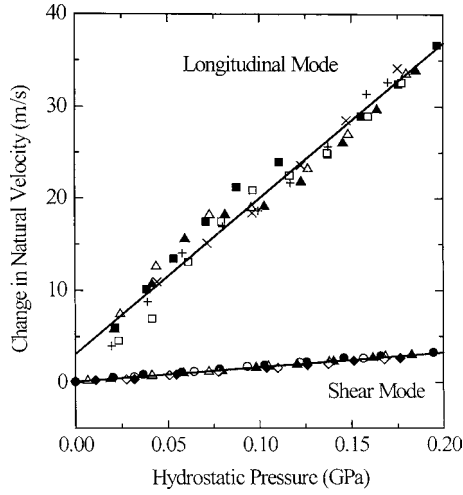


Figure 4 Hydrostatic-pressure dependence of the change in natural velocity for the longitudinal and shear modes, measured at room temperature for ceramic α -Mo₂C. The filled symbols correspond to measurements made with increasing pressure and the open symbols to data as the pressure was decreased (different symbols refer to different experimental runs). The straight lines are the least-squares fits to the experimental data.

ultrasonic velocity measurements under pressure by using [43]

$$\left(\frac{\partial M}{\partial P}\right)_{P=0} = (M)_{P=0} \left[\frac{2(\partial f/\partial P)}{f} + \frac{1}{3B^T} \right]_{P=0}, \quad (4)$$

where B^T is the isothermal bulk modulus, f is the pulse-echo overlap frequency at atmospheric pressure and $\partial f/\partial P$ is its pressure derivative. The adiabatic bulk modulus B^S has been used rather than B^T throughout the calculations: a procedure, which introduces only a negligible error. The hydrostatic-pressure derivatives $(\partial C_L/\partial P)_{P=0}$, $(\partial \mu/\partial P)_{P=0}$ and $(\partial B^S/\partial P)_{P=0}$ determined for ceramic α -Mo₂C have positive values (Table I). Both the longitudinal and shear elastic stiffnesses and thus the slopes of the corresponding acoustic mode dispersion curves, at the long-wavelength limit, increase with pressure. The value obtained for the hydrostatic-pressure derivative $(\partial \mu/\partial P)_{P=0}$ of the shear stiffness for ceramic α -Mo₂C is typical for a stiff solid and similar to those found [44] for ceramic TiC and TaC whose pore fractions are smaller than the α -Mo₂C ceramic used in this work. This indicates that the value obtained for $(\partial \mu/\partial P)_{P=0}$ of ceramic α -Mo₂C is not greatly influenced by the highly porous nature of the sample. However, the values determined for the hydrostatic-pressure derivatives $(\partial C_L/\partial P)_{P=0}$ and $(\partial B^S/\partial P)_{P=0}$ of ceramic α -Mo₂C are very large when compared to those found [44] for the TiC and TaC ceramics.

It is known that the porous microstructure of ceramics affects the hydrostatic-pressure induced changes in ultrasonic wave velocities and hence the pressure derivative $(\partial B^S/\partial P)_{P=0}$ of the bulk modulus (see for instance [35]). In the absence of experimental data for the effects of pressure on the elastic stiffness tensor components of single-crystal α -Mo₂C, it is not possible at present to separate the intrinsic from defect contributions to

$(\partial B^S/\partial P)_{P=0}$ for ceramic α -Mo₂C. However, it is instructive to compare the value determined in this study for $(\partial B^S/\partial P)_{P=0}$ of ceramic α -Mo₂C with those obtained by other researchers using other methods. Haines *et al.* [10] performed X-ray powder diffraction measurements on α -Mo₂C under quasi-hydrostatic pressure conditions up to 46 GPa at room temperature and analysed the data on the pressure dependence of the unit cell volume in terms of the Birch-Murnaghan equation of state. They determined a value of 6.5 for the pressure derivative $(\partial B^T/\partial P)$ of the isothermal bulk modulus of α -Mo₂C. This value and that ($=4.34$) obtained from *ab-initio* calculations [10] are much smaller than that (Table I) determined here for the hydrostatic-pressure derivative $(\partial B^S/\partial P)_{P=0}$ of the adiabatic bulk modulus of ceramic α -Mo₂C. This comparison indicates that specimen porosity and the defect microstructure of α -Mo₂C [7, 19] have substantial influence on the determination of the effects of hydrostatic pressure on the volume-dependent elastic stiffness (C_L) and adiabatic bulk modulus (B^S) of its ceramic form. However, it should also be noted that, at the high pressures (>2 GPa) involved in the diamond anvil cell experiments the unit cell volume is substantially reduced. The isothermal bulk modulus (B^T) reported by Haines *et al.* [10] corresponds to the enhanced value for a material under high compression, which enhances the bulk modulus and in addition causes $\partial B^T/\partial P$ to be a pressure-dependent quantity, decreasing with increasing pressure [45].

The bulk modulus and its hydrostatic pressure derivative (Table I) have been used to calculate the volume compression $V(P)/V_0$ of ceramic α -Mo₂C up to very high pressures, using an extrapolation method based on the Murnaghan's equation of state [46] in the logarithmic form. The calculations have been performed at room temperature and results are shown in Fig. 5. The volume compression of ceramic α -Mo₂C is in reasonable agreement with that obtained from high pressure X-ray powder diffraction experiments [10].

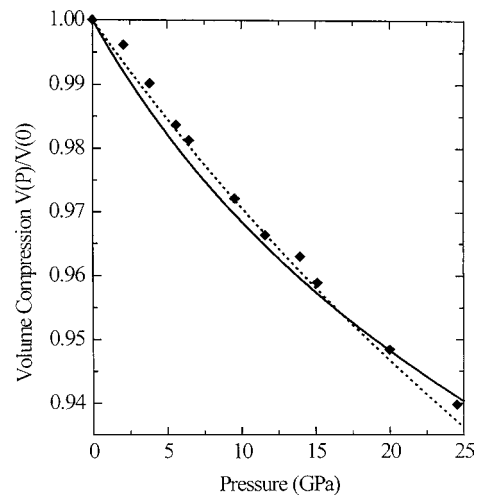


Figure 5 Volume compression of ceramic α -Mo₂C (full line) at room temperature extrapolated to very high pressures, using Murnaghan's equation of state [46], in comparison with the very high pressure X-ray powder diffraction data for α -Mo₂C (full diamonds and dotted line) taken from [10].

6. Conclusions

The velocities of longitudinal and shear 10 MHz ultrasonic waves, propagated in a hot-pressed α -Mo₂C ceramic, have been measured as functions of temperature and hydrostatic pressure. The α -Mo₂C ceramic is a comparatively stiff material elastically; the longitudinal elastic stiffness and the adiabatic bulk modulus of this ceramic are large. The bulk modulus is in accord with the strong interatomic bonding in this material. The shear elastic stiffness and Young's modulus show normal behaviour with temperature and can be fitted to the conventional model for lattice vibrational anharmonicity. The longitudinal elastic stiffness and bulk modulus increase with decreasing temperature and show a knee at about 200 K, below which longitudinal acoustic-mode softening occurs. The hydrostatic-pressure derivative of the shear stiffness has a small value typical for transition metal carbides, while the hydrostatic-pressure derivatives of the longitudinal elastic stiffness and bulk modulus have large positive values, possibly due to the defect microstructure of the ceramic.

Acknowledgments

We would like to thank Professor George A. Saunders for his continuous support during the work, and E. F. Lambson, W. A. Lambson and R. C. J. Draper for technical assistance. B. J. is grateful to MOD for Corporate Research Programme funding.

References

1. L. E. TOTH, "Transition Metal Carbides and Nitrides" (Academic Press, New York, 1971).
2. P. ETTMAYER and W. LENGAUER, "Encyclopedia of Inorganic Chemistry" (Wiley, New York, 1994) p. 519.
3. S. T. OYAMA, in "Transition Metal Carbides and Nitrides: Application of Transition Metal Carbides and Nitrides in Industrial Tools," edited by S. T. Oyama (Blackie Acad. and Prof., London, 1996) p. 1.
4. F. W. CLINARD, JR. and C. P. KEMPTER, *J. Less-Common Metals*, **15** (1968) 59.
5. A. E. MARTINELLI, R. A. L. DREW and R. BERRICHE, *J. Mater. Sci. Lett.* **15** (1996) 306.
6. E. LUCAZEAU, A. DENEUVILLE, J. FONTENILLE, F. BRUNET and E. GHEERAERT, *Diam. Relat. Mater.* **5** (1996) 779.
7. E. RUDY, ST. WINDISCH, A. J. STOSICK and J. R. HOFFMAN, *Trans. Metall. Soc. AIME* **239** (1967) 1247.
8. J. DUBOIS, T. EPICIER, C. ESNOUF, G. FANTOZZI and P. CONVERT, *Acta Metall.* **36** (1988) 1891.
9. T. EPICIER, J. DUBOIS, C. ESNOUF, G. FANTOZZI and P. CONVERT, *ibid.* **36** (1988) 1903.
10. J. HAINES, J. M. LÉGER, C. CHATEAU and J. E. LOWTHER, *J. Phys.: Condens. Matter* **13** (2001) 2447.
11. W. KÖSTER and R. RAUSCHER, *Z. Metallkunde* **39** (1948) 111.
12. G. V. SAMSONOV and K. I. PORTNOY, "Alloys Based on High-Melting Compounds" (Gosudarstvenoye Nauchno-Tekhnicheskoye Izdatel'stvo Oborongiz, Moscow, 1961) p. 181.
13. P. T. B. SHAFFER, "Handbook of High Temperature Materials" (Plenum Press, New York, 1964) p. 99.

14. J. F. LYNCH, C. G. RUDERER and W. M. DUCKWORTH (eds.), in "Engineering Properties of Selected Ceramic Materials" (American Ceramic Society, Inc., Ohio, 1966).
15. I. N. FRANTSEVICH, E. A. ZHURAKOVSKII and A. B. LYASHCHENKO, *Inorg. Mater.* **3** (1967) 6.
16. C. KRAL, W. LENGAUER, D. RAFAJA and P. ETTMAYER, *J. Alloys Comp.* **265** (1998) 215.
17. L. E. TOTH, J. ZBASNIK, Y. SATO and W. GARDNER, in Proceedings of International Symposium on Anisotropy in Single-Crystal Refractory Compounds (Dayton, Ohio, June 1967), edited by F. W. Vahldiek and S. A. Mersol (Plenum Press, New York, 1968) Vol. 1, p. 249.
18. F. W. VAHLDIEK, S. A. MERSOL and C. T. LYNCH, *Trans. Metall. Soc. AIME* **236** (1966) 1490.
19. F. W. VAHLDIEK and S. A. MERSOL, in Proceedings of International Symposium on Anisotropy in Single-Crystal Refractory Compounds (Dayton, Ohio, June 1967), edited by F. W. Vahldiek and S. A. Mersol (Plenum Press, New York, 1968) Vol. 1, p. 199.
20. L. E. TOTH and J. ZBASNIK, *Acta Metall.* **16** (1968) 1177.
21. Y. A. CHANG, L. E. TOTH and Y. S. TYAN, *Metall. Trans.* **2** (1971) 315.
22. H. STUART and N. RIDLEY, *J. Iron. St. Inst.* **208** (1970) 1087.
23. M. YAMASHITA, *J. Phys. E: Sci. Instrum.* **20** (1987) 1457.
24. L. C. DY and W. S. WILLIAMS, *J. Appl. Phys.* **53** (1982) 8915.
25. W. S. WILLIAMS, *Int. J. Refract. Met. Hard Mater.* **17** (1999) 21.
26. F. A. MODINE, M. D. FOEGELLE, C. B. FINCH and C. Y. ALLISON, *Phys. Rev. B* **40** (1989) 9558.
27. C. H. HINRICHS, M. H. HINRICHS and W. A. MACKIE, *J. Appl. Phys.* **68** (1990) 3401.
28. E. P. PAPADAKIS, *J. Acoust. Soc. Amer.* **42** (1967) 1045.
29. E. KITTINGER, *Ultrasonics* **15** (1977) 30.
30. R. N. THURSTON and K. BRUGGER, *Phys. Rev.* **133** (1964) A1604.
31. C. M. SAYERS and R. L. SMITH, *Ultrasonics* **20** (1982) 201.
32. M. CANKURTARAN, G. A. SAUNDERS, J. R. WILLIS, A. AL-KHEFFAJI and D. P. ALMOND, *Phys. Rev. B* **39** (1989) 2872.
33. L. D. LANDAU and E. M. LIFSHITZ, "Theory of Elasticity," 3rd ed. (Pergamon Press, Oxford, 1986).
34. O. L. ANDERSON, *J. Phys. Chem. Solids* **24** (1963) 909.
35. Q. WANG, G. A. SAUNDERS, D. P. ALMOND, M. CANKURTARAN and K. C. GORETTA, *Phys. Rev. B* **52** (1995) 3711.
36. P. LLOYD and M. V. BERRY, *Proc. Phys. Soc.* **91** (1967) 678.
37. D. L. PRICE and B. R. COOPER, *Phys. Rev. B* **39** (1989) 4945.
38. H. W. HUGOSSON, O. ERIKSSON, L. NORDSTRÖM, U. JANSSON, L. FAST, A. DELIN, J. M. WILLS and B. JOHANSSON, *J. Appl. Phys.* **86** (1999) 3758.
39. R. H. J. HANNINK and M. J. MURRAY, *J. Mater. Sci.* **9** (1974) 223.
40. S. C. LAKKAD, *J. Appl. Phys.* **42** (1971) 4277.
41. S. P. DODD, M. CANKURTARAN, G. A. SAUNDERS and B. JAMES, *J. Mater. Sci.* **36** (2001) 2557.
42. H. G. SMITH and W. GLASER, *Phys. Rev. Lett.* **25** (1970) 1611.
43. R. N. THURSTON, *Proc. IEEE* **53** (1965) 1320.
44. S. P. DODD, M. CANKURTARAN and B. JAMES, *J. Mater. Sci.* **38** (2003) 1107.
45. C. FANGGAO, M. CANKURTARAN, G. A. SAUNDERS, A. AL-KHEFFAJI, D. P. ALMOND and P. J. FORD, *Supercond. Sci. Technol.* **4** (1991) 13.
46. F. D. MURNAGHAN, *Proc. Natl. Acad. Sci. USA* **30** (1944) 244.

Received 14 April
and accepted 22 October 2003